Project: **620**

Project title: **Multiskalen-Simulationen mit EULAG and PMAP**

Principal investigator: **Andreas Dörnbrack**

Report period: **2024-11-01 to 2025-10-31**

Part 1: Gravity Wave Drag and Momentum and Energy Fluxes Across the Mountain Wave Spectrum: Contrasting Linear Analytic Solutions and Nonlinear Numerical Simulations

This section of the report sketches the main results of Binder et al. (2025), a paper just submitted to the Journal of Atmospheric Sciences. It comprises two overarching goals. (1) Contrasting the results of idealized numerical simulations of different mountain wave regimes with linear analytic solutions of the surface gravity wave drag (GWD). (2) A comparison and validation of two different numerical models, the Portable Model for multi-scale Atmospheric Prediction (PMAP, Krieger 2024) and the predecessor of its dynamical core, the EUlerian/semi-LAGrangian flow solver (EULAG). While EULAG utilizes Levante's CPU cores, PMAP can be set up utilizing CPU or GPU cores. The latter has been used on Levante for all the presented PMAP simulations.

In the first part, the key result is that nonlinear numerical simulations reproduce the principal characteristics of the analytical solutions across all mountain wave regimes. In Figure 1, the markers (nonlinear numerical simulations) closely follow the grey/black lines (linear analytic solutions by Blumen, 1965, Smith, 1979, Miranda and James, 1992). Systematic deviations arise in transitional cases where non-hydrostatic and rotational effects overlap. Since both factors decrease the overall surface GWD, it is plausible that the GWD in these transitional regimes is smaller in simulations than in linear theories, which are only valid for one or the other approximation. The numerical experiments showed that simulations with an axisymmetric (circular) mountain rather than a two-dimensional ridge underestimate the surface GWD, particularly for narrower mountains (in non-hydrostatic regimes), likely due to partial flow splitting not captured by the analytical formulations. Furthermore, tests with periodic lateral boundary conditions indicate a suppression of the Coriolis effect, leading to higher simulated surface GWD for larger mountain widths than in an open-boundary configuration.

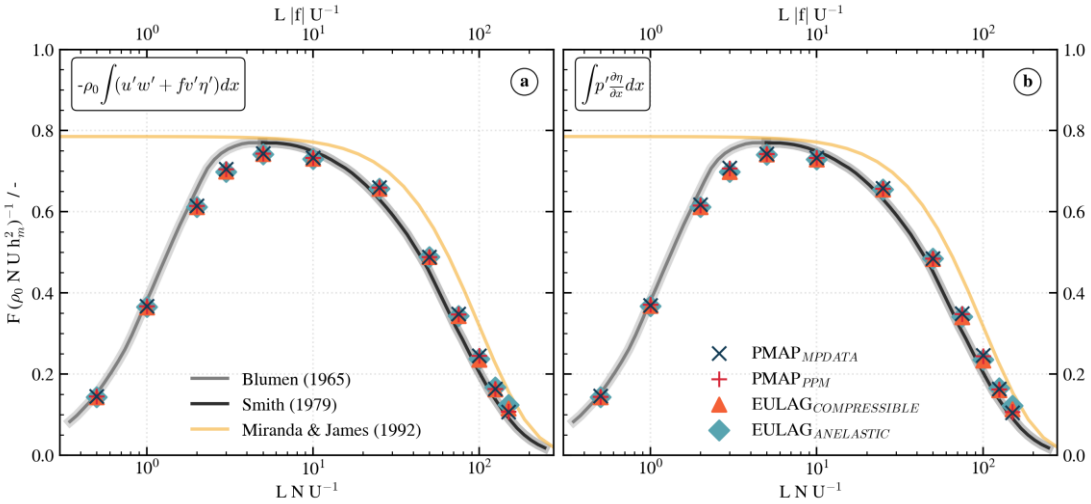

Figure 1: Both panels compare results of nonlinear numerical simulations (markers) with linear analytic solutions (grey, black and yellow lines) for the normalized surface GWD for a flow over a Witch of Agnesi mountain. The surface GWD can be calculated via the vertical flux of angular momentum shown in panel (a) and via its fundamental definition using the pressure perturbations shown in panel (b). The x-axis spans the range of mountain wave regimes. Buoyancy frequency $N = 0.01$ s^{-1} and flow speed $u_e = 10$ m s^{-1}, and the Coriolis frequency $f = 0.01$ N are uniform, so only the mountain half-width L increases from left to right. 12 mountain wave regimes from L = 0.5 km to L = 150 km have been simulated. Different markers refer to different model configurations: PMAP_MPDATA, PMAP_PPM, EULAG_COMPRESSIBLE, and EULAG_ANELASTIC.

To extend the analysis of surface quantities into the vertical structure of the flow, we introduced a diagnostic method to compute the vertical flux of angular momentum throughout the model domain, assuming an adiabatic flow along isentropes. In this context, zonal-mean profiles of momentum and energy fluxes were found to closely satisfy the Eliassen–Palm relation and highlight distinct differences between low- and high-frequency mountain wave regimes (Eliassen and Palm, 1961). For example, the zonal energy flux EF_x and the total energy E_0 show a similar pattern as the surface GWD in Figure 1. They peak in the hydrostatic mountain wave regime (L = 5-10km) and decrease for both smaller and larger mountain half-widths.

The main conclusion of the paper's second part is that discrepancies between the two numerical models (EULAG and PMAP), between two different advection schemes (MPDATA and PPM), and between the compressible Euler equations and their anelastic approximation are small compared to the differences between the nonlinear simulations and linear theories. Different markers in Figure 1 closely overlap across all mountain regimes, so varying the model setup results in minor discrepancies in the surface values compared to the difference between the simulations and the linear solutions represented by the solid lines.

Altogether, these are encouraging results that enable us to smoothly transition from CPU-based to GPU-based computing systems using the new PMAP model.

Part 2: Numerical simulations of gravity wave breaking and secondary gravity waves above the Southern Andes

The second part of this report briefly summarizes the progress of high-resolution numerical simulations to investigate the propagation of gravity waves above the Southern Andes in the presence of tides (transient background conditions) and their appearance in different measurements. Simulations with an isotropic resolution of 800 m have already demonstrated that numerical experiments will significantly improve the interpretation of our ground-based Rayleigh temperature lidar CORAL measurements. We will continue this research as planned, aiming for a combination of simulations using a larger domain and slightly coarser resolution, and simulations with a 400 m resolution on a smaller domain. The latter will also be used to address another research topic triggered by recent CORAL observations. These suggest that large-amplitude, high-frequency temperature perturbations observed in the measurements between 50 and 60 km are related to gravity wave breaking and, potentially, the formation of vortex rings. Preliminary simulations with EULAG on Levante, using a 400 m grid spacing, indicate that vortex rings could indeed explain these large temperature perturbations. Additional resources have been requested to extend the analysis and tackle this topic specifically.

References (bold names are members of the project):

Binder, M., Dörnbrack, A., Krieger, N., Kühnlein, C., 2025. Gravity Wave Drag and Momentum and Energy Fluxes Across the Mountain Wave Spectrum: Contrasting Linear Analytic Solutions and Nonlinear Numerical Simulations. *J. Atmos. Sci*., under review.

Blumen, W., 1965: Momentum Flux by Mountain Waves in a Stratified Rotating Atmosphere. *J. Atmos. Sci.*, **22**, 529–534, https://doi.org/10.1175/1520-0469(1965)022<0529:MFBMWI>2.0.CO;2.

Eliassen, A., and E. Palm, 1961: On the Transfer of Energy in Stationary Mountain Waves. *Geofys. Publ.,* **22**, 1-23.

Krieger, N., 2024: Large-eddy simulations with PMAP and applications to a local Alpine windstorm. Ph.D. thesis, ETH Zurich, https://doi.org/10.3929/ethz-b-000719398

Miranda, P. M. A. and James, I. N., 1992: Non-Linear Three-Dimensional Effects On Gravity-Wave Drag: Splitting Flow and Breaking Waves. *Q.J.R. Meteorol. Soc*., **118**, 1057-1081. https://doi.org/10.1002/qj.49711850803

Smith, R., 1979: The Influence of the Earth's Rotation on Mountain Wave Drag. *J. Atmos. Sci.*, **36**, 177–180, https://doi.org/10.1175/1520-0469(1979)036<0177:TIOTER>2.0.CO;2.